HHS Public Access

Author manuscript

Nat Chem. Author manuscript; available in PMC 2018 July 01.

Published in final edited form as:

Nat Chem. 2017 July ; 9(7): 667–675. doi:10.1038/nchem.2706.

A synthetic ion transporter that disrupts autophagy and induces apoptosis by perturbing cellular chloride concentrations

Nathalie Busschaert[1,†,‡], **Seong-Hyun Park**[2,‡], **Kyung-Hwa Baek**[2], **Yoon Pyo Choi**[2], **Jinhong Park**[3], **Ethan N. W. Howe**[1,†], **Jennifer R. Hiscock**[1,†], **Louise E. Karagiannidis**[1], **Igor Marques**[4], **Vítor Félix**[4], **Wan Namkung**[3], **Jonathan L. Sessler**[5,*], **Philip A. Gale**[1,*,†], and **Injae Shin**[2,*]

[1]Chemistry, University of Southampton, Southampton SO17 1BJ, UK

[2]Department of Chemistry, Yonsei University, 03722 Seoul, Korea

[3]College of Pharmacy, Yonsei Institute of Pharmaceutical Sciences, Yonsei University, 21983 Incheon, Korea

[4]Department of Chemistry, CICECO – Aveiro Institute of Materials, Department of Medical Sciences, iBiMED – Institute of Biomedicine, University of Aveiro, 3810-193, Aveiro, Portugal

[5]Department of Chemistry, University of Texas at Austin, 78712-1224 Austin, Texas, USA

Abstract

Perturbations in cellular chloride concentrations can affect cellular pH and autophagy and lead to the onset of apoptosis. With this in mind, synthetic ion transporters have been used to disturb cellular ion homeostasis and thereby induce cell death; however, it is not clear whether synthetic ion transporters can also be used to disrupt autophagy. Here, we show that squaramide-based ion transporters enhance the transport of chloride anions in liposomal models and promote sodium chloride influx into the cytosol. Liposomal and cellular transport activity of the squaramides is shown to correlate with cell death activity, which is attributed to caspase-dependent apoptosis. One ion transporter was also shown to cause additional changes in lysosomal pH, which leads to

* sessler@cm.utexas.edu; philip.gale@sydney.edu.au; injae@yonsei.ac.kr.

†Present addresses: Silver Center for Arts and Science, New York University, Department of Chemistry, 100 Washington Square East, New York, New York 10003, USA (N.B.); School of Chemistry, University of Sydney, NSW 2006, Australia (E.N.W.H., P.A.G.); School of Physical Sciences, University of Kent, Park Wood Road, Canterbury, Kent CT2 7NH, UK (J.R.H.).

‡These authors contributed equally to this work.

Data availability. Data collected in Southampton have been made available online at http://dx.doi.org/10.5258/SOTON/402335 to comply with the EPSRC open data policy. Other data are available from the authors on request.

Author contributions

I.S. and N.B. designed the study and wrote the manuscript. J.L.S. and P.A.G. helped with writing the manuscript. I.S., J.L.S and P.A.G. supervised the project. S.-H.P., K.-H.B. and Y.P.C. performed biological studies. N.B. designed, synthesized and characterized the compounds and performed the ion-transport studies in liposomes and the anion binding studies. E.N.W.H., J.R.H. and L.E.K. helped with some of the liposomal studies. I.M. and V.F. carried out DFT calculations and $V_{s,max}$ calculations. J.P. and W.N. carried out ion-transport activity studies in cells.

Additional information

Supplementary information is available in the online version of the paper. Correspondence and requests for materials should be addressed to J.L.S., P.A.G. and I.S.

Competing financial interests

The authors declare no competing financial interests.

impairment of lysosomal enzyme activity and disruption of autophagic processes. This disruption is independent of the initiation of apoptosis by the ion transporter. This study provides the first experimental evidence that synthetic ion transporters can disrupt both autophagy and induce apoptosis.

Autophagy is a self-eating process that contributes to cell survival under starvation conditions[1], and the discoveries of mechanisms for autophagy were recognized by this year's Nobel Prize in Physiology or Medicine[2,3]. During autophagy, subcellular organelles and other cell components are sequestered in double-membrane vesicles (autophagosomes) and are delivered to lysosomes for digestion and recycling. It is known that levels of autophagy in cancer cells are generally higher than those in normal cells[4], leading to suggestions that autophagy-disrupting agents may be potentially useful in the treatment of cancers[5,6].

Apoptosis—programmed cell death—is an intrinsic self-killing process that is necessary for maintaining tissue homeostasis[6]. Multiple previous studies have served to demonstrate that tumour cells are resistant to apoptotic cell death via multiple anti-apoptotic processes[7]. Thus, much effort has been made to discover potent apoptosis inducers that can be used as anticancer agents[8,9]. One approach that we have explored recently involves the use of ion transporters to disrupt cellular ion homeostasis[10].

Normally, the extracellular chloride concentration (~120 mM) is much higher than the cytosolic chloride concentration (5–40 mM)[11]. These concentrations are maintained through the action of transmembrane ion transporters and channels[12]. It is known that the dysregulation of intracellular concentrations of ions, particularly chloride anions, correlates closely with the onset of apoptosis[13]. Physiological perturbations in cellular chloride concentrations can also affect pH and autophagy[14]. Lysosomal pH values are typically maintained at <5.0 by sustaining a ~80 mM lysosomal chloride concentration through the action of the lysosomal chloride transporters[11]. When the lysosomal chloride concentration is decreased to the level where the lysosomal pH exceeds 5.0 (refs[11,15]), the activity of the lysosomal enzymes required for the digestion of biomolecules is reduced, leading to autophagy disruption. These observations lead us to suggest that synthetic ion transporters, which modulate cytosolic and lysosomal chloride concentrations and pH and consequently induce apoptosis and disrupt autophagy, may have a role to play as antitumour pharmaceuticals.

The effect of ion transporters on autophagy has not been investigated. However, several carrier systems have been reported that induce apoptosis. For instance, prodigiosin (a naturally occurring small-molecule-based ion transporter) and its analogues are known to induce cancer cell death by altering intracellular pH gradients through HCl transport[16–18]. Recently, we found that a synthetic diamide-strapped calix[4]pyrrole **1** (Fig. 1a), which promotes an influx of Cl^- and Na^+ into cells, enhances cell death via caspase-dependent apoptosis[10]. Interestingly, bis-(*p*-nitrophenyl) ureidodecalin **2** (Fig. 1a) has been shown to function as an anion transporter without affecting cell viability[19].

In an effort to determine the effects of perturbing ion homeostasis on organelle and cell function, we carried out a comparative study involving the known chloride-transporting mono-squaramide **3** (ref.[20]) and a series of related mono-, bis- and tris-squaramides **4**–**8** (Fig. 1b). Tripodal squaramide systems analogous to **7** and **8** were reported to possess interesting anion-binding properties[21], while urea and thiourea analogues of **4**–**8** were found to be highly active anion transporters with cytotoxic activity[22–24]. These compounds were therefore expected to function as potent anion transporters with biological activity. As detailed in the following, several transporters promote apoptosis, while squaramide **3** also serves to increase the lysosomal pH, leading to autophagy disruption. To our knowledge, this is the first time that a synthetic ion transporter has been shown to affect the function of a subcellular organelle.

Results and discussion

Ion transport activity of synthetic squaramides in a liposome model

To test whether compounds **3**–**8** act as effective ion transporters, unilamellar 1-palmitoyl-2-oleoyl-*sn*-glycero-3-phosphocholine (POPC) vesicles containing 489 mM NaCl with 5 mM sodium phosphate (pH 7.2) were prepared according to standard procedures[20]. The vesicles were suspended in a 489 mM external $NaNO_3$ solution with 5 mM sodium phosphate (pH 7.2), and chloride efflux induced by the addition of a DMSO solution of **3**–**8** (1 mol% w.r.t. lipid) was monitored using a chloride-selective electrode. As shown in Fig. 2a, compound **3** transported all of the chloride anions from the vesicles within ~120 s, while **7** and **8** were inactive. Measurements of the initial rate of chloride transport (k_{ini}, Fig. 1b) revealed a transport activity order of **3** > **5** > **6** > **4** ≫ **7** ~ **8** (or **3** > **5** > **4** ≫ **7** and **6** > **8** when the squaramides are classified in a *para*-CF_3 and *meta*-CF_3 series, respectively; Fig. 1b). This conclusion was confirmed by concentration-dependent anion transport assays (Supplementary Tables 4–7). Similar experiments, with the chloride-containing vesicles suspended in external Na_2SO_4 or $NaHCO_3$ solutions, provided evidence that the squaramides are capable of Cl^-/NO_3^- transport (Fig. 2a and Supplementary Fig. 49), Cl^-/HCO_3^- transport (Supplementary Figs 26 and 49) and, to a lesser extent, Cl^-/SO_4^{2-} transport (Supplementary Figs 32–42 and 49). Assays using the pH-sensitive dye 8-hydroxypyrene-1,3,6-trisulfonic acid, trisodium salt[25,26] revealed that squaramides **3**–**6** can dissipate a pH gradient, presumably through H^+/Cl^- symport or Cl^-/OH^- antiport (Supplementary Figs 44–47). In contrast, a ^{23}Na NMR spectroscopic study revealed that the squaramides are unable to transport Na^+ ions effectively across POPC bilayers at pH 7.2 (Supplementary Figs 33–35). Tripodal compounds **7** and **8** were found to be inactive transporters.

The poor transport ability of **7** and **8** is surprising given the potent anion transport activity of the corresponding urea/thiourea analogues[23]. Lipophilicity, which determines the ability of a compound to partition into the membrane, has been linked to transmembrane anion transport activity[22,27]; however, no clear correlation[28] between lipophilicity and anion transport with these compounds could be found (Supplementary Fig. 97a). We thus sought to find a relationship between the anion transport and anion affinity of the squaramides. In DMSO-d_6/0.5% water (Supplementary Table 8 and Figs 68–95), the bis- and tris-squaramides **5**–**8**

displayed 1:2 receptor–anion binding stoichiometries. This results in highly charged complexes that would be unable to diffuse through a nonpolar lipid bilayer.

Given the above, we calculated the most positive values of the surface electrostatic potential of **3**–**8** ($V_{s,max}$, Fig. 2b, inset), a descriptor that has been shown to correlate strongly with hydrogen bond donating ability[29] and anion binding[22]. Figure 2b shows a plot of the initial rate of transport (k_{ini}) as a function of $V_{s,max}$. The bell-shaped plot, with **3** at the maximum, leads us to suggest that some compounds interact too weakly with anions to allow efficient chloride transport (low $V_{s,max}$, compound **4**), while others bind anions too strongly (high $V_{s,max}$, compounds **7**–**8**). Anion transport requires both the uptake of the anion on one side of the membrane and release of the anion on the other side of the membrane. A 'Goldilocks' effect in terms of binding and transport has thus often been suggested for anion transporters[30,31]. Transporter **3** appears to embody this effect.

We next sought to determine whether the receptor-mediated ion transport occurs in an electrogenic or electroneutral fashion. Electrogenic transport implies the net movement of a charged species (for example, Cl^- alone), which creates a membrane potential that can be compensated by a separate electrogenic transport event (for example, the transport of another anion or cation). During electroneutral processes, no net transfer of charge occurs and the transport of the two ions (one cation and one anion, or two different anions) cannot be separated. Using a recently developed method[32,33], and exploiting both valinomycin (an electrogenic K^+ transporter)[34] and monensin (an electroneutral M^+/H^+ transporter)[35], we conclude that **3** is capable of both electrogenic Cl^- transport and electroneutral H^+/Cl^- (OH^-/Cl^-) transport (Fig. 2c,d). Bis-squaramides **5** and **6** appeared to be significantly more efficient in mediating electroneutral H^+/Cl^- (OH^-/Cl^-) transport than electrogenic Cl^- transport (Supplementary Figs 50 and 51). No selectivity for the transport of Cl^- over H^+ (or OH^-) is seen for **3**, **5** or **6** (Supplementary Table 7).

Cellular ion transport and cell death activities of synthetic squaramides

As a first test of whether the synthetic squaramides **3**–**8** could act as ion transporters in cells, their ability to promote changes in cytosolic chloride concentrations was assessed, in analogy to what has been done previously[10]. Briefly, Fischer rat thyroid epithelial (FRT) cells, stably expressing a mutant yellow fluorescent protein (YFP-F46L/H148Q/I152L) whose fluorescence is quenched sensitively by chloride ions, were incubated with each compound. Based on the extent of fluorescence quenching, the relative chloride transport activity in cells (cf. Fig. 3a and Supplementary Fig. 98a) was found to mirror what was found in the liposomal studies, namely **3** > **5** > **4** ≫ **7** for *para*-CF_3 compounds and **6** > **8** for *meta*-CF_3 compounds (Fig. 1b). Because FRT cells lack endogenous chloride channels/transporters, we can exclude the possibility that the chloride ion influx is the result of natural chloride channels/transporters.

We then determined which cations, if any, entered the cells treated with the synthetic squaramides **3**–**8**. In an initial study, changes in intracellular sodium concentrations were measured by treating FRT cells with the sodium fluorescent probe SBFI-AM (sodium-binding benzofuran isophthalate acetoxymethyl ester) followed by treatment with **3**–**8**

(ref.[10]). It was found that while **3**, **5** and **6** are effective in increasing the intracellular sodium concentration, compounds **4**, **7** and **8** have little or no effect (Fig. 3b and Supplementary Fig. 98b). On the basis of an amiloride sodium channel inhibition study[10], we conclude that transporters **3**, **5** and **6** function mainly as electrogenic chloride anion transporters and that the sodium counter-ions enter cells in a concomitant fashion through cellular sodium channels (Fig. 3a,b). This is in agreement with what is observed in the liposome models for the coupling of **3** with valinomycin (Fig. 2d).

In contrast to what proved true for sodium ions, the intracellular potassium and calcium concentrations remain unchanged upon incubation, as inferred from experiments using potassium (PBFI-AM; potassium-binding benzofuran isophthalate acetoxymethyl ester) and calcium (Fluo-4) fluorescent probes (Supplementary Fig. 99)[10]. Such findings are consistent with the relatively low extracellular concentrations of potassium (4 mM versus 145 mM for Na^+) and calcium (1.5 mM) and the unfavourable gradients that might be expected in the case of K^+ (intracellular concentration = 150 mM)[13]. These findings provide support for the notion that transporters **3**, **5** and **6** function as chloride anion transporters in conjunction with channel-mediated sodium cation co-transport (Supplementary Fig. 100).

An increase in cytosolic chloride concentrations is known to induce cell death[10,36]. We thus investigated the effect of squaramides **3**–**8** on cell viability. HeLa (human cervical cancer cells) and A549 cells (human lung carcinoma epithelial cells) were incubated with each compound at various concentrations. An MTT (3-(4,5-dimethylthiazol-2-yl)-2,5-diphenyltetrazolium bromide) assay was used to measure cell viabilities. It was found that **3**, **5** and **6**, with good ion transport activity in cells, effectively induce cell death, but **4**, **7** and **8**, with little or no ion transport activity in cells, have a very low effect on cell death (Supplementary Fig. 101). The half maximum inhibitory concentration (IC_{50}) values of **3**, **5** and **6** were determined in several cancer cell lines (HeLa, A549, PLC/PRF/5 (hepatocellular carcinoma cells) and HepG2 (hepatoblastoma cells)) and were found to vary from 2 to 6 μM (Fig. 1b and Supplementary Fig. 102).

To examine whether the observed synthetic transporter-induced cell death results from increased concentrations of chloride and sodium ions in cells, the effect of extracellular Cl^- and Na^+ on cell death induced by **3**, **5** and **6** was determined[10,37]. HeLa and A549 cells were incubated with various concentrations of each compound in buffers containing both chloride and sodium ions (HEPES-buffered solutions) or in analogous buffers depleted in either chloride anions (Cl^--free solutions) or sodium cations (Na^+-free solutions). As expected for an ion transport-based effect, the cell death activity of **3**, **5** and **6** was reduced in both the Cl^--free and Na^+-free media (Supplementary Fig. 103).

HeLa and A549 cells were also incubated with **3**, **5** and **6** in the presence of various non-toxic concentrations of amiloride. A considerable decrease in cell death activity was seen (Supplementary Fig. 104). This finding is consistent with the notion that the cell death mediated by **3**, **5** and **6** relies in large measure on endogenous sodium ion channels to assure charge balance.

Synthetic transporters promote apoptosis

Multiple previous studies have served to show that dysregulation of ion homeostasis, particularly via chloride influx, can induce apoptosis[10,36,38]. To test if the present synthetic transporters accelerate apoptosis, HeLa and A549 cells were separately exposed to **3**, **5** and **6**, as well as FCCP (carbonyl cyanide 4-(trifluoromethoxy)phenylhydrazone), a control apoptosis inducer that depolarizes mitochondrial membranes[39]. The cells were then treated with a mixture of fluorescein-labelled annexin V and propidium iodide (PI). The results of flow cytometry analysis showed that cells treated with **3**, **5** or **6**, as well as FCCP, display positive annexin V binding and PI uptake (Fig. 3c and Supplementary Figs 105a and 106a). The finding indicates that **3**, **5** and **6** have apoptosis-inducing activity. Analysis of cell size by flow cytometry revealed that cells treated with **3**, **5** and **6** as well as FCCP exhibit a considerable degree of cell shrinkage (Supplementary Figs 105b, 106b and 107). This finding also serves to rule out cell death via necrosis as a dominant mechanism, because necrosis normally leads to cell swelling. The loss of mitochondrial membrane potential, a hallmark of apoptosis, was further investigated using a membrane-potential-sensitive probe JC-1 (ref.[8]). The results of fluorescence activated cell sorting (FACS) analysis revealed an increase in JC-1 green fluorescence and a decrease in red fluorescence in cells treated with **3**, **5**, **6** or FCCP, as would be expected for apoptosis (Fig. 3d and Supplementary Figs 105c and 106c)[40]. An increase in DNA fragmentation was also observed in cells treated with **3**, **5**, **6** or FCCP (Supplementary Figs 106d and 108). Finally, cells incubated with **3** were subjected to gene expression profiling analysis of mRNAs using human DNA chips. Analysis of DNA chip data shows that a number of positive regulators of apoptosis are upregulated more than twofold compared to an untreated control, whereas expression levels of negative regulators of apoptosis are downregulated (Supplementary Table 10). Taken together, these results provide clear evidence that cells treated with synthetic transporters **3**, **5** and **6** undergo apoptosis, but not necrosis.

Synthetic transporters induce caspase-dependent apoptosis

To test whether transporters **3**, **5** and **6** induce caspase-dependent apoptosis[41], HeLa and A549 cells were incubated with each compound at various concentrations. The caspase activities of the treated cell lysates were then determined by using a colorimetric peptide substrate for caspases, Ac-DEVD-pNA (pNA, *p*-nitroaniline). They were found to increase in cells treated with **3**, **5** or **6** (Fig. 4a and Supplementary Fig. 109a). On the other hand, almost no caspase activity was seen when Ac-DEAD-CHO, a known inhibitor of caspases, was added to the lysates of cells treated with **3**, **5** or **6**.

During caspase-dependent apoptosis, cytochrome *c* is released from the mitochondria into the cytosol, where it associates with Apaf-1 to form the apoptosome[42]. The apoptosome complex activates caspase-9, which subsequently leads to caspase-3 activation through the cleavage of procaspase-3 (ref.[42]). In tests carried out with HeLa and A549 cells, cytochrome *c* release into the cytosol and the generation of cleaved caspase-3 were seen after incubation with **3**, **5** or **6** (Fig. 4b and Supplementary Fig. 109b). Additional experiments, aimed at evaluating cleavage of a cellular caspase substrate, poly(ADP-ribose) polymerase (PARP), revealed that the cleaved product of PARP is generated in cells treated with **3**, **5** or **6**.

The apoptosis inducing factor (AIF) is typically translocated into the nucleus during caspase-independent apoptosis[43]. The level of AIF in the nucleus was thus examined after incubating HeLa and A549 cells with **3**, **5** or **6**. No appreciable transport of AIF translocation into the nucleus was observed (Supplementary Fig. 110). These results support the conclusion that transporters **3**, **5** and **6** promote caspase activation but not AIF-associated, caspase-independent apoptosis.

To evaluate whether ion influx promoted by transporters **3**, **5** and **6** is a cause or a consequence of apoptosis, HeLa cells were incubated with each compound at different time periods and then treated with the sodium fluorescent probe SBFI-AM, the Cl^--quenching fluorescent probe MQAE (*N*-(ethoxycarbonylmethyl)-6-methoxy-quinolinium bromide)[10,44], the membrane potential sensitive probe JC-1 and fluorescein–annexin V. These studies revealed that sodium chloride transport into cells takes place shortly after incubation with **3**, **5** or **6** (Fig. 4c,d). However, increases in JC-1 green fluorescence and annexin V positive cells (indicators of apoptosis[45]) occur at later times (Fig. 4e and Supplementary Fig. 111). We thus conclude that ion influx is the likely cause of apoptosis, rather than apoptosis leading to changes in ion flux, as might be expected if **3**, **5** and **6** were operating via a non-transport mechanism.

Synthetic transporter 3 increases lysosomal pH and impairs lysosomal enzyme activity

Dysregulation of intracellular chloride concentrations can lead to suppression of cell proliferation via autophagy disruption by altering the lysosomal pH and impairing lysosomal enzyme activity[14,46]. Autophagy starts with engulfment of cytoplasmic constituents by the phagophore, which is then expanded to form the double-membrane autophagosome (Supplementary Fig. 112). The autophagosome subsequently fuses with the lysosome to generate the autolysosome. Degradation requires lysosomal enzymes, whose activities are maximal at low pH ($pH \leq 5$)[47]. The lysosomal pH is known to be correlated with chloride anion concentrations, which in turn are regulated by lysosomal chloride transporters[14,48]. Higher pH values are correlated with relatively lower lysosomal chloride anion concentrations. Because the lysosomal chloride concentrations are higher (~80 mM) than cytosolic chloride concentrations (5–40 mM)[11], a lysosomal membrane-permeable chloride ion transporter might be expected to disrupt the autophagic process by promoting the transfer of chloride anions and therefore H^+ out of the lysosome.

To examine whether synthetic transporters **3**, **5** and **6** affect the lysosomal pH, HeLa cells, pretreated with fluorescein-tetramethylrhodamine-tagged dextran (a ratiometric lysosomal pH indicator[49]), were separately incubated with **3**, **5** and **6**, along with a control **8**. Treatment with **3** leads to an increase in the lysosomal pH to ~7.0. In contrast, a lysosomal pH of less than 5.0 was measured in cells treated with **5**, **6** or **8** (Fig. 5a and Supplementary Figs 113 and 114). Although we could not determine the lysosomal chloride concentration directly owing to the lack of appropriate probes, the pH-modulation results suggest that **3** decreases the lysosomal chloride anion concentrations under conditions where the other systems, namely **5**, **6** and **8**, do not.

Because the lysosomal pH increases when cells are treated with **3**, we anticipated that this transporter would suppress lysosomal enzyme activities. To test this, we determined the activity of cathepsins B and L, which are critical enzymes that degrade proteins in lysosomes during autophagy, by using cell-permeable fluorogenic peptide substrates MR-$(RR)_2$ and MR-$(FR)_2$, respectively[50]. The intact probes are nonfluorescent, but once the respective peptide moiety attached to the probes is cleaved by the action of lysosomal cathepsins B and L, a red fluorescent dye accumulates in the cytoplasm. HeLa cells treated with **3**, **5** or **6** were thus separately incubated with MR-$(RR)_2$ or MR-$(FR)_2$. As a control the cells were also treated with leupeptin, an inhibitor of serine and cysteine proteases, followed by incubation of MR-$(RR)_2$ or MR-$(FR)_2$. Confocal microscopy image analysis revealed that cells treated with **5** or **6** exhibit strong red fluorescence signals in analogy to untreated cells, but cells treated with **3** or leupeptin are characterized by a significantly attenuated red fluorescence (Fig. 5b). We thus conclude that **3** increases the lysosomal pH, leading to reduction in cathepsin B and L activity.

Transporter 3 disrupts the autophagic process

Because cathepsin B and L activity was disrupted by **3**, we anticipated that **3** (but not **5** or **6**) would impair the autophagic process in cells. The microtubule-associated protein 1 light chain 3-II (LC3-II) and p62 are often used to monitor autophagy[5]. Typically, increased levels of LC3-II and decreased levels of p62 are observed during autophagy induction. In contrast, the levels of both LC3-II and p62 are increased when autophagic flux is disrupted. HeLa cells were thus incubated with **3**, as well as **5** and **6**. Torin-1 and bafilomycin A1 (BfA1) were used as controls for autophagy induction and inhibition, respectively. Increased levels of both LC3-II and p62 were seen in cells treated with **3** compared to untreated cells (Fig. 5c and Supplementary Fig. 115a). Such an increase was also observed in cells treated with the autophagy inhibitor BfA1. In contrast, LC3-II and p62 levels in cells treated with **5** and **6** were similar to those in untreated cells. As expected, cells treated with torin-1 were characterized by an increase in the LC3-II level and a decrease in the p62 level.

HeLa cells, stably expressing a tandem mRFP-EGFP-LC3 fusion protein (mRFP, monomeric red fluorescence protein; EGFP, enhanced green fluorescence protein), were also incubated with **3**, **5** and **6**, as well as torin-1 and BfA1. It is known that both RFP and GFP fluorescence signals are observed in the autophagosome. Typically, RFP but not GFP signals are seen in the acidic autolysosome[51]. Confocal microscopy image analysis of HeLa cells treated with **3** revealed a conspicuous increase in yellow vesicles, reflecting a merger of the GFP and RFP fluorescence emission signals (Fig. 5d and Supplementary Fig. 115b). This phenomenon was also observed in BfA1-treated cells. In contrast, cells treated with torin-1 display mainly red fluorescent vesicles, a finding that is indicative of autolysosome formation. Cells treated with **5** and **6** displayed fluorescence patterns similar to those of untreated cells (Supplementary Fig. 116). On this basis, we conclude that autolysosomes are not being formed in cells treated with **3**. Rather, we suggest that transporter **3** increases the lysosomal pH, disrupts lysosomal cathepsin activity in cells and, as a consequence, impairs the autophagic process.

Transporters **3**, **5** and **6** all display good chloride ion transport activity at the lysosomal pH (≤5.0), as inferred from liposomal studies carried out at pH 7.2 and 4.0 (Supplementary Fig. 48). We thus believe that the different bioactivity of these three transporters reflects the fact that **3** moves to the lysosome efficiently. In contrast, **5** and **6** are transported into cells but are unable to leave the cell plasma membranes and reach the lysosomes due to their high lipophilicity (Supplementary Table 9) or their potential to bind strongly to the phospholipid headgroups (high *V*s,max, Supplementary Table 9). This is a very specific manifestation of the Goldilocks effect noted above.

Autophagy disruption and apoptosis induction by 3 take place via independent pathways

To determine whether the autophagy disruption and apoptosis induced by **3** are linked, HeLa cells were incubated with **3** in the absence and presence of a cell-permeable pan-caspase inhibitor ZVAD-FMK (benzyloxycarbonyl-Val-Ala-Asp-fluoromethylketone)[52]. Caspase activation promoted by **3** was almost completely suppressed in the presence of ZVAD-FMK (Supplementary Fig. 117). However, ZVAD-FMK itself has no influence on the autophagic process (Fig. 6a,b). Cells co-treated with **3** and ZVAD-FMK displayed similar levels of LC3-II and p62 when compared to those in cells treated with **3** alone. HeLa cells stably expressing mRFP-EGFP-LC3 were also treated with either **3** alone or co-treated with **3** and ZVAD-FMK. Similar mRFP puncta co-localized with EGFP were seen in both cases (Fig. 6b and Supplementary Fig. 118). Further studies were carried out using BfA1. This substance is an inhibitor of vacuolar H^+ ATPase, which blocks autophagy by impairing lysosomal acidification and fusion of autophagosomes with lysosomes[53]. In contrast to **3**, treatment with BfA1 alone does not promote caspase-dependent apoptosis. On the other hand, HeLa cells co-treated with **3** and BfA1 undergo apoptosis to a similar degree when compared with cells treated with **3** alone (Fig. 6c–e). Finally, we examined the time dependence of the apoptosis induction and autophagy disruption produced by **3**. An increase in the levels of LC3 and p62, as well as the appearance of co-localized puncta of mRFP with EGFP, were observed at early times after treatment of cells with **3** (Supplementary Fig. 119). On the other hand, apoptosis promoted by **3** took place at later times (Fig. 4e). Collectively, the findings indicate that the autophagy disruption induced by **3** precedes apoptosis and occurs independently.

Conclusions

On the basis of the findings presented here we propose that transporter **3** (but not **5** or **6**) mediates its observed autophagy impairment function by promoting chloride transport. This leads to an increase in lysosomal pH, which results in impairment of activity of lysosomal enzymes critical for the degradation of biomolecules during autophagy. This disrupts the autophagic process (cf. Supplementary Fig. 120). Independent of its effect on the lysosomes, the increase in cytosolic sodium cations and chloride anions mediated by **3** (as well as **5** and **6**) results in cytochrome *c* release from the mitochondria into the cytosol, promoting caspase-dependent apoptosis. As a consequence, transporter **3** promotes the induction of apoptosis as well as disrupting autophagy. We thus suggest that synthetic ion transporters, such as **3**, which promote apoptosis and inhibit autophagy, may in due course find a role as anticancer agents.

Supplementary Material

Refer to Web version on PubMed Central for supplementary material.

Acknowledgments

This study was supported financially by the National Creative Research Initiative (grant no. 2010-0018272 to I.S.) and Basic Science Research programmes (grant no. NRF-2012R1A1A1040142 to W.N.) in Korea. P.A.G. acknowledges the EPSRC for postdoctoral fellowships (EP/J009687/1 to N.B. and E.N.W.H.) and the Royal Society and the Wolfson Foundation for a Research Merit Award. The work in Austin was supported by the National Institutes of Health (grant no. GM103790 to J.L.S.). The theoretical studies were supported by projects P2020-PTDC/QEQ-SUP/4283/2014, CICECO – Aveiro Institute of Materials (UID/CTM/50011/2013) and iBiMED – Institute of Biomedicine (UID/BIM/04501/2013), financed by National Funds through the FCT/MEC and co-financed by QREN-FEDER through COMPETE under the PT2020 Partnership Agreement. I.M. acknowledges the FCT for PhD scholarship SFRH/BD/87520/2012. The authors thank H.J. Clarke for resynthesizing compound **5**.

References

1. Mizushima N, Komatsu M. Autophagy: renovation of cells and tissues. Cell. 2011; 147:728–741. [PubMed: 22078875]
2. Ohsumi Y. Molecular dissection of autophagy: two ubiquitin-like systems. Nat Rev Mol Cell Biol. 2001; 2:211–216. [PubMed: 11265251]
3. Kuma A, et al. The role of autophagy during the early neonatal starvation period. Nature. 2004; 432:1032–1036. [PubMed: 15525940]
4. White E. Deconvoluting the context-dependent role for autophagy in cancer. Nat Rev Cancer. 2012; 12:401–410. [PubMed: 22534666]
5. Baek KH, Park J, Shin I. Autophagy-regulating small molecules and their therapeutic applications. Chem Soc Rev. 2012; 41:3245–3263. [PubMed: 22293658]
6. Newmeyer DD, Ferguson-Miller S. Mitochondria: releasing power for life and unleashing the machineries of death. Cell. 2003; 112:481–490. [PubMed: 12600312]
7. Igney FH, Krammer PH. Death and anti-death: tumour resistance to apoptosis. Nat Rev Cancer. 2002; 2:277–288. [PubMed: 12001989]
8. Williams DR, Ko SK, Park S, Lee MR, Shin I. An apoptosis-inducing small molecule that binds to heat shock protein 70. Angew Chem Int Ed. 2008; 47:7466–7469.
9. Ko SK, et al. A small molecule inhibitor of ATPase activity of HSP70 induces apoptosis and has antitumor activities. Chem Biol. 2015; 22:391–403. [PubMed: 25772468]
10. Ko SK, et al. Synthetic ion transporters can induce apoptosis by facilitating chloride anion transport into cells. Nat Chem. 2014; 6:885–892. [PubMed: 25242483]
11. Stauber T, Jentsch TJ. Chloride in vesicular trafficking and function. Annu Rev Physiol. 2013; 75:453–477. [PubMed: 23092411]
12. Gould D. Human physiology: From cells to systems, 3rd edition. J Adv Nurs. 1998; 28:680–682.
13. Yu SP, Canzoniero LMT, Choi DW. Ion homeostasis and apoptosis. Curr Opin Cell Biol. 2001; 13:405–411. [PubMed: 11454444]
14. Hosogi S, Kusuzaki K, Inui T, Wang X, Marunaka Y. Cytosolic chloride ion is a key factor in lysosomal acidification and function of autophagy in human gastric cancer cell. J Cell Mol Med. 2014; 18:1124–1133. [PubMed: 24725767]
15. Anke D, et al. CFTR regulates phagosome acidification in macrophages and alters bactericidal activity. Nat Cell Biol. 2006; 8:933–944. [PubMed: 16921366]
16. Sessler JL, et al. Synthesis, anion-binding properties, and *in vitro* anticancer activity of prodigiosin analogues. Angew Chem Int Ed. 2005; 117:6143–6146.
17. Ohkuma S, et al. Prodigiosins uncouple lysosomal vacuolar-type ATPase through promotion of H^+/Cl^- symport. Biochem J. 1998; 334:731–741. [PubMed: 9729483]
18. Melvin MS, et al. Double-strand DNA cleavage by copper·prodigiosin. J Am Chem Soc. 2000; 122:6333–6334.

19. Li H, et al. Efficient, non-toxic anion transport by synthetic carriers in cells and epithelia. Nat Chem. 2016; 8:24–32. [PubMed: 26673261]
20. Busschaert N, et al. Squaramides as potent transmembrane anion transporters. Angew Chem Int Ed. 2012; 51:4426–4430.
21. Jin C, et al. Squaramide-based tripodal receptors for selective recognition of sulfate anion. Chem Commun. 2013; 49:2025–2027.
22. Busschaert N, et al. Towards predictable transmembrane transport: QSAR analysis of anion binding and transport. Chem Sci. 2013; 4:3036–3045.
23. Busschaert N, et al. Structure–activity relationships in tripodal transmembrane anion transporters: the effect of fluorination. J Am Chem Soc. 2011; 133:14136–14148. [PubMed: 21846096]
24. Moore SJ, et al. Chloride, carboxylate and carbonate transport by ortho-phenylenediamine-based bisureas. Chem Sci. 2013; 4:103–117.
25. Clement NR, Gould JM. Pyranine (8-hydroxy-1,3,6-pyrenetrisulfonate) as a probe of internal aqueous hydrogen ion concentration in phospholipid vesicles. Biochemistry. 1981; 20:1534–1538. [PubMed: 6261798]
26. Busschaert N, et al. Thiosquaramides: pH switchable anion transporters. Chem Sci. 2014; 5:3617–3626. [PubMed: 26146535]
27. Valkenier H, Haynes CJE, Herniman J, Gale PA, Davis AP. Lipophilic balance – a new design principle for transmembrane anion carriers. Chem Sci. 2014; 5:1128–1134.
28. Li Z, Deng LQ, Chen JX, Zhou CQ, Chen WH. Does lipophilicity affect the effectiveness of a transmembrane anion transporter? Insight from squaramido-functionalized bis(choloyl) conjugates. Org Biomol Chem. 2015; 13:11761–11769. [PubMed: 26488550]
29. Hagelin H, Murray JS, Politzer P, Brinck T, Berthelot M. Family-independent relationships between computed molecular surface quantities and solute hydrogen bond acidity/basicity and solute-induced methanol O–H infrared frequency shifts. Can J Chem. 1995; 73:483–488.
30. Behr JP, Kirch M, Lehn JM. Carrier-mediated transport through bulk liquid membranes: dependence of transport rates and selectivity on carrier properties in a diffusion-limited process. J Am Chem Soc. 1985; 107:241–246.
31. Vargas Jentzsch A, et al. Ditopic ion transport systems: anion–π interactions and halogen bonds at work. Angew Chem Int Ed. 2011; 50:11675–11678.
32. Wu X, et al. Nonprotonophoric electrogenic chloride transport mediated by valinomycin-like carriers. Chem. 2016; 1:127–146.
33. Howe ENW, et al. pH-regulated nonelectrogenic anion transport by phenylthiosemicarbazones. J Am Chem Soc. 2016; 138:8301–8308. [PubMed: 27299473]
34. Läuger P. Mechanisms of biological ion transport—carriers, channels, and pumps in artificial lipid membranes. Angew Chem Int Ed. 1985; 24:905–923.
35. Mollenhauer HH, James Morré D, Rowe LD. Alteration of intracellular traffic by monensin; mechanism, specificity and relationship to toxicity. Biochim Biophys Acta. 1990; 1031:225–246. [PubMed: 2160275]
36. Tsukimoto M, Harada H, Ikari A, Takagi K. Involvement of chloride in apoptotic cell death induced by activation of ATP-sensitive P2 × 7 purinoceptor. J Biol Chem. 2005; 280:2653–2658. [PubMed: 15550367]
37. Bortner CD, Cidlowski JA. Uncoupling cell shrinkage from apoptosis reveals that Na^+ influx is required for volume loss during programmed cell death. J Biol Chem. 2003; 278:39176–39184. [PubMed: 12821680]
38. Saha T, Hossain MS, Saha D, Lahiri M, Talukdar P. Chloride-mediated apoptosis-inducing activity of bis(sulfonamide) anionophores. J Am Chem Soc. 2016; 138:7558–7567. [PubMed: 27222916]
39. Waterhouse NJ, et al. Cytochrome *c* maintains mitochondrial transmembrane potential and ATP generation after outer mitochondrial membrane permeabilization during the apoptotic process. J Cell Biol. 2001; 153:319–328. [PubMed: 11309413]
40. Tzung SP, et al. Antimycin A mimics a cell-death-inducing Bcl-2 homology domain 3. Nat Cell Biol. 2001; 3:183–191. [PubMed: 11175751]

41. Elmore S. Apoptosis: a review of programmed cell death. Toxicol Pathol. 2007; 35:495–516. [PubMed: 17562483]
42. Li P, et al. Cytochrome *c* and dATP-dependent formation of Apaf-1/caspase-9 complex initiates an apoptotic protease cascade. Cell. 1997; 91:479–489. [PubMed: 9390557]
43. Joza N, et al. Essential role of the mitochondrial apoptosis-inducing factor in programmed cell death. Nature. 2001; 410:549–554. [PubMed: 11279485]
44. Cho HJ, et al. A small molecule that binds to an ATPase domain of Hsc70 promotes membrane trafficking of mutant cystic fibrosis transmembrane conductance regulator. J Am Chem Soc. 2011; 133:20267–20276. [PubMed: 22074182]
45. Perelman A, et al. JC-1: alternative excitation wavelengths facilitate mitochondrial membrane potential cytometry. Cell Death Dis. 2012; 3:e430. [PubMed: 23171850]
46. Yang YP, et al. Application and interpretation of current autophagy inhibitors and activators. Acta Pharmacol Sin. 2013; 34:625–635. [PubMed: 23524572]
47. Xie Z, Klionsky DJ. Autophagosome formation: core machinery and adaptations. Nat Cell Biol. 2007; 9:1102–1109. [PubMed: 17909521]
48. Graves AR, Curran PK, Smith CL, Mindell JA. The Cl^-/H^+ antiporter ClC-7 is the primary chloride permeation pathway in lysosomes. Nature. 2008; 453:788–792. [PubMed: 18449189]
49. DiCiccio JE, Steinberg BE. Lysosomal pH and analysis of the counter ion pathways that support acidification. J Gen Physiol. 2011; 137:385–390. [PubMed: 21402887]
50. Creasy BM, Hartmann CB, White FKH, McCoy KL. New assay using fluorogenic substrates and immunofluorescence staining to measure cysteine cathepsin activity in live cell subpopulations. Cytometry Part A. 2007; 71A:114–123.
51. Kimura S, Noda T, Yoshimori T. Dissection of the autophagosome maturation process by a novel reporter protein, tandem fluorescent-tagged LC3. Autophagy. 2007; 3:452–460. [PubMed: 17534139]
52. Chen Y, McMillan-Ward E, Kong J, Israels SJ, Gibson SB. Oxidative stress induces autophagic cell death independent of apoptosis in transformed and cancer cells. Cell Death Differ. 2007; 15:171–182. [PubMed: 17917680]
53. Jahreiss L, Menzies FM, Rubinsztein DC. The itinerary of autophagosomes: from peripheral formation to kiss-and-run fusion with lysosomes. Traffic. 2008; 9:574–587. [PubMed: 18182013]

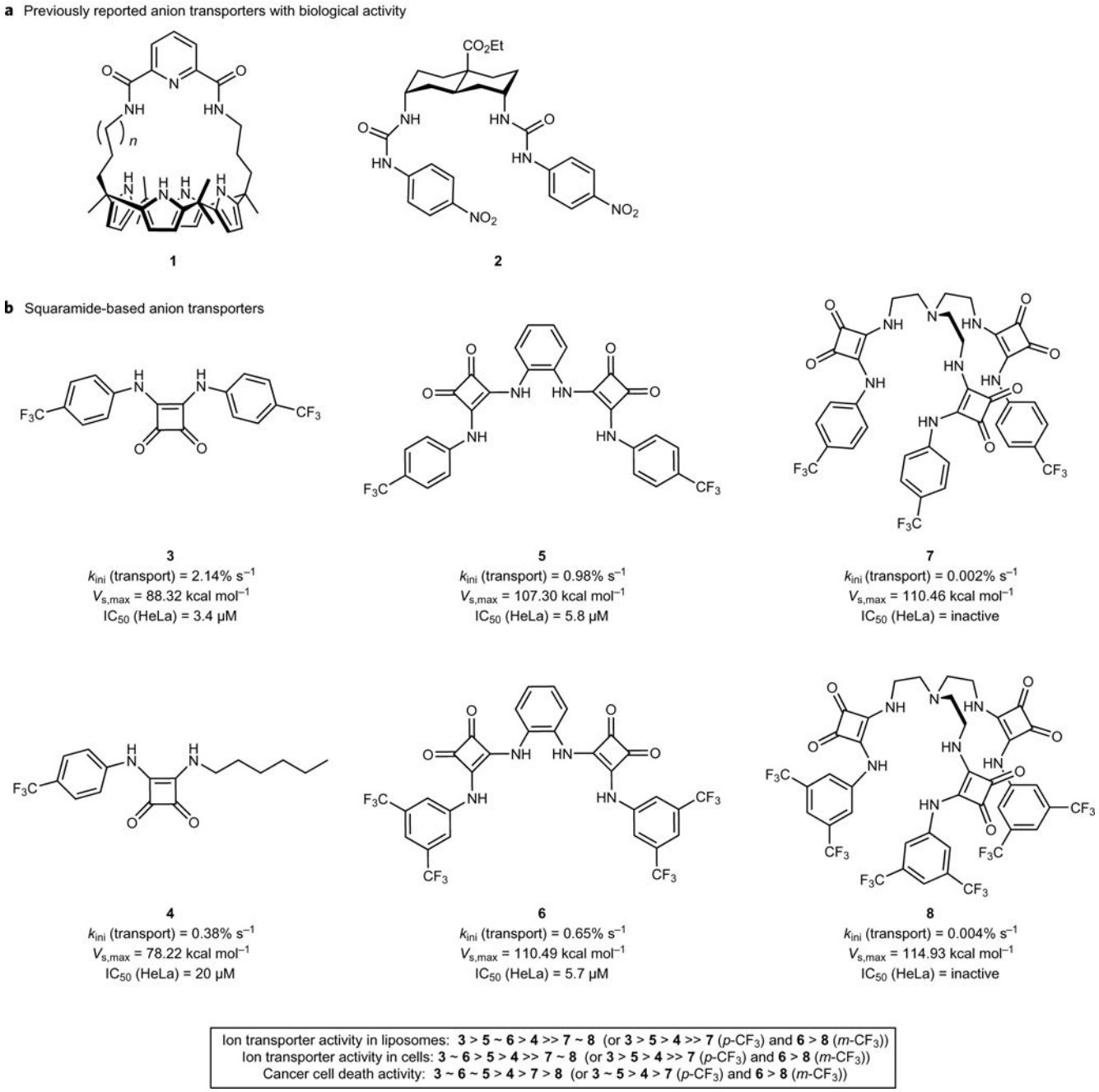

Figure 1. Structure of anion transporters and their activity

a, Structures of previously reported anion transporters **1** and **2**. **b**, Structures of squaramide-based anion transporters **3**–**8** and the initial rate of chloride transport mediated by 1 mol% transporter from liposomes filled with a buffered NaCl solution and submerged in a buffered $NaNO_3$ solution (k_{ini}), calculated $V_{s,max}$ values, and IC_{50} values towards HeLa cells. Inset: relative activity (from high to low) for the various transporters in different assays.

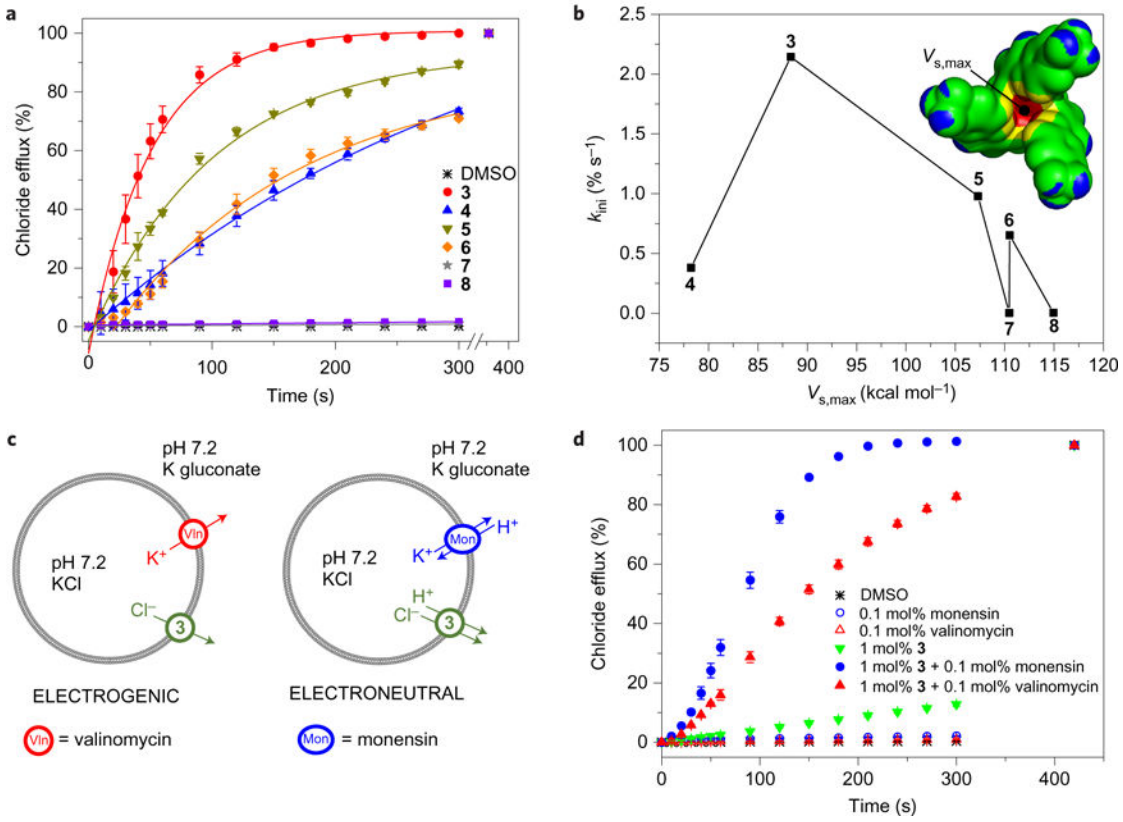

Figure 2. Ion transport studies using liposomal model membranes

a, Cl^-/NO_3^- antiport mediated by **3**–**8** (added as DMSO solutions; final concentration: 1 mol % w.r.t. lipid) from POPC vesicles loaded with 489 mM NaCl with 5 mM phosphate salts (pH 7.2) and suspended in a 489 mM $NaNO_3$ solution with 5 mM phosphate salts (pH 7.2). Error bars represent standard deviations from three separate experiments, and lines correspond to the initial rate of transport (k_{ini}) calculations. **b**, Plot representing the correlation between the initial rate of transport (k_{ini}) and $V_{s,max}$. Inset: surface electrostatic potential with $V_{s,max}$ of compound **7** (colour scale, from blue to red (in kcal mol^{-1}): blue, lower than −7.5; green, between −7.5 and 40.0; yellow, between 40.0 and 87.5; red, greater than 87.5). **c**, Experimental set-up to determine electrogenic or electroneutral anion transport. POPC vesicles are loaded with 300 mM KCl with 5 mM phosphate salts (pH 7.2) and suspended in a 300 mM potassium gluconate solution with 5 mM phosphate salts (pH 7.2). Electrogenic K^+ transport by valinomycin can only occur if it is balanced by electrogenic Cl^- transport by **3**. Electroneutral K^+/H^+ antiport by monensin can only occur if the pH gradient is dissipated by electroneutral H^+/Cl^- transport by **3**. **d**, Results of the experiment described in **c**, showing both electrogenic and electroneutral anion transport by squaramide **3**. Transporters are added as DMSO solutions to start the experiments (resulting in a final concentrations of 0.1 mol% w.r.t. lipid for valinomycin and monensin, and 1 mol% w.r.t. lipid for squaramide **3**). Error bars represent standard deviations from three separate experiments.

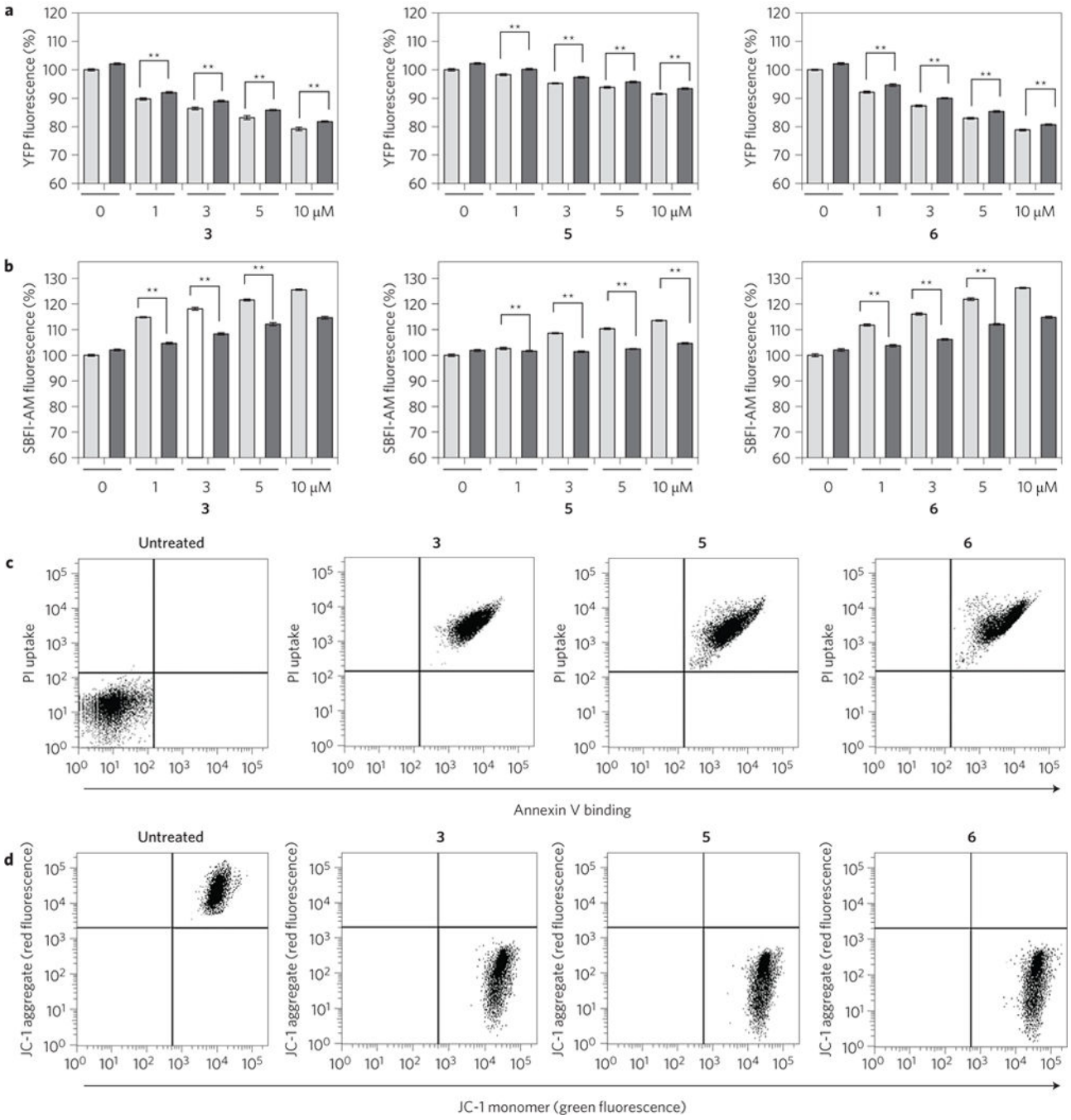

Figure 3. Synthetic transporters induce apoptosis

a, FRT cells stably transfected with a mutant YFP gene were incubated with various concentrations of the indicated compounds for 2 h in the absence (grey bars) and presence (black bars) of 1 mM amiloride. YFP fluorescence was then measured to examine changes in intracellular chloride ion concentrations (mean ± s.d., $n = 3$, $^{**}P < 0.001$, Student's *t*-test). **b**, FRT cells pretreated with 10 μM SBFI-AM for 1.5 h were incubated with various concentrations of the indicated compounds for 2 h in the absence (grey bars) and presence (black bars) of 1 mM amiloride. SBFI-AM fluorescence was then measured to examine

changes in intracellular sodium ion concentrations (mean ± s.d., $n = 3$, $^{**}P < 0.001$, Student's *t*-test). **c**, Flow cytometry of HeLa cells treated with 10 μM of indicated compounds for 18 h and stained with fluorescein-annexin V and PI (annexin V binding versus PI uptake). Untreated cells are shown as a negative control. **d**, Flow cytometry of HeLa cells treated with 10 μM of indicated compounds for 18 h and stained with JC-1 (red fluorescence (FL2, JC-1 aggregate) versus green fluorescence (FL1, JC-1 monomer)). Untreated cells are shown as a negative control.

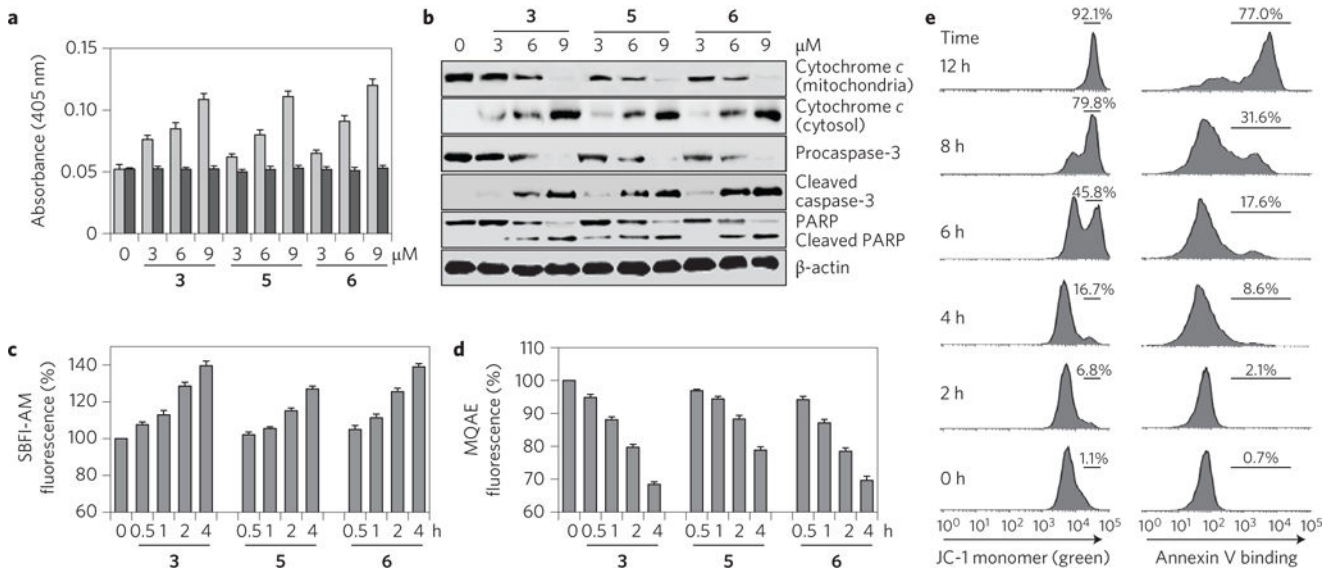

Figure 4. Synthetic transporters induce caspase-dependent apoptosis

a, Caspase activities of lysates of HeLa cells treated with the indicated compounds for 18 h were measured by using 200 μM acetyl-DEVD-pNA in the absence (grey bars) and presence (black bars) of 20 μM Ac-DEVD-CHO (mean ± s.d., $n = 3$). **b**, HeLa cells were treated with the indicated compounds for 18 h. Immunoblotting was conducted using the corresponding antibodies. β-Actin was used as a loading control. **c**, HeLa cells pretreated with 10 μM SBFI-AM were incubated with 10 μM of the indicated compounds for the indicated times. The SBFI-AM fluorescence was then measured to probe changes in the intracellular sodium ion concentration (mean ± s.d., $n = 3$). **d**, HeLa cells pretreated with 10 mM MQAE for 1 h were incubated with 10 μM of each compound for the indicated times. The MQAE fluorescence was then measured to determine changes in the intracellular chloride ion concentration (mean ± s.d., $n = 3$). **e**, Flow cytometry of HeLa cells treated with 10 μM **3** for the indicated time and then stained with JC-1 (left) or fluorescein-annexin V (right).

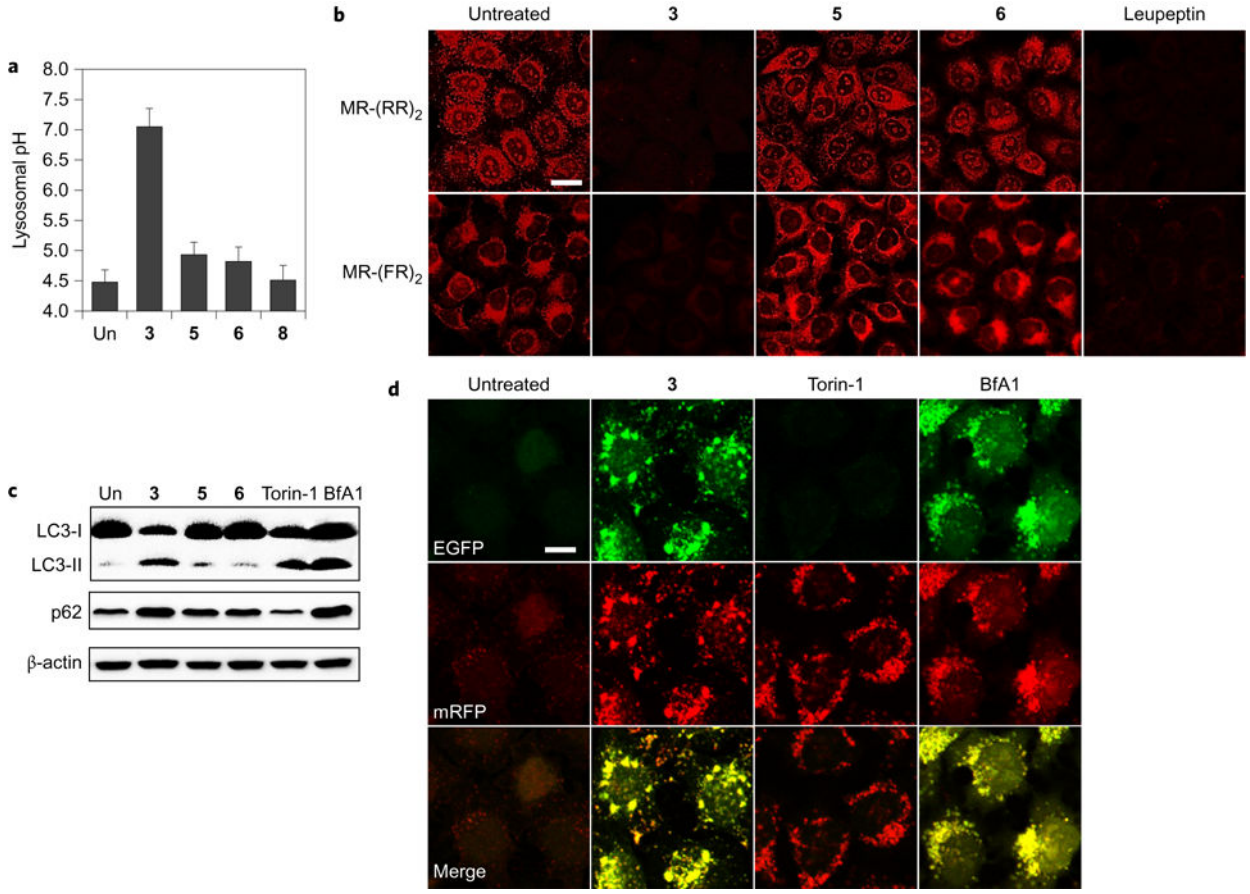

Figure 5. Effect of synthetic transporters on autophagy

a, HeLa cells pretreated with fluorescein-tetramethylrhodamine-tagged dextran for 12 h were incubated with 10 μM of the indicated compounds for 12 h. The lysosomal pHs were calculated using a pH titration curve (shown in Supplementary Fig. 113) (mean ± s.d., n = 3). **b**, HeLa cells pretreated with **3** (4 μM), **5** (4 μM), **6** (4 μM) or leupeptin (5 μM) for 6 h were incubated with MR-$(RR)_2$ or MR-$(FR)_2$ for 4 h. Cell images were obtained using confocal fluorescence microscopy (scale bar, 20 μm). **c**, HeLa cells were treated with **3** (4 μM), **5** (4 μM), **6** (4 μM), torin-1 (1 μM) or BfA1 (5 nM) for 24 h. Expression levels of LC3 and p62 were examined using western blots. Torin-1 and BfA1 were used as controls for autophagy induction and inhibition, respectively. **d**, HeLa cells stably expressing mRFP-EGFP-LC3 were treated with **3** (4 μM), torin-1 (1 μM) or BfA1 (5 nM) for 24 h. Cell images were obtained using confocal fluorescence microscopy (scale bar, 10 μm).

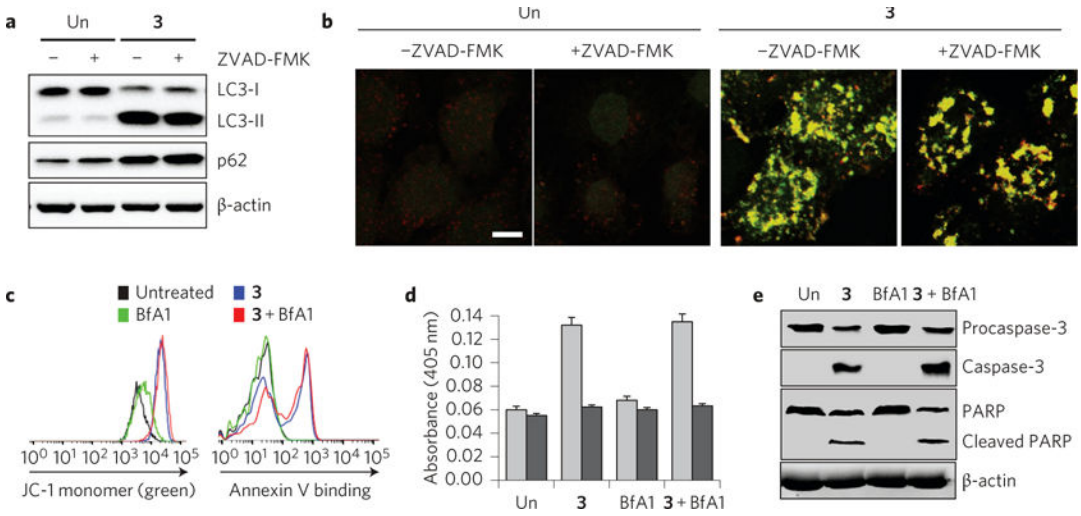

Figure 6. Effect of apoptosis induction promoted by 3 is independent of its ability to disrupt autophagy

a, HeLa cells were treated for 12 h with 10 μM **3** in the absence and presence of 40 μM ZVAD-FMK. The indicated proteins were immunoblotted using the corresponding antibodies. 'Un' indicates no treatment of cells with **3**. **b**, HeLa cells stably expressing mRFP-EGFP-LC3 were treated for 24 h with 10 μM **3** in the absence and presence of 40 μM ZVAD-FMK. Cell images of EGFP and mRFP, obtained using confocal fluorescence microscopy, were merged (scale bar, 10 μm). 'Un' indicates no treatment of cells with **3**. **c**, Flow cytometry of HeLa cells treated with 10 μM **3** or/and 5 nM BfA1 for 12 h and then stained with JC-1 (left) or fluorescein-annexin V (right). 'Untreated' indicates no treatment of cells with **3** and BfA1. **d**, Caspase activities of lysates of HeLa cells treated with 10 μM **3** or/and 5 nM BfA1 for 12 h were measured using 200 μM acetyl-DEVD-pNA in the absence (grey bars) and presence (black bars) of 20 μM Ac-DEVD-CHO (mean ± s.d., $n = 3$). 'Un' indicates no treatment of cells with **3** and BfA1. **e**, HeLa cells were treated with 10 μM **3** or/and 5 nM BfA1 for 12 h. The indicated proteins were then immunoblotted by using the corresponding antibodies. 'Un' indicates no treatment of cells with **3** and BfA1.